

## High-pressure study of isoviolanthrone by Raman spectroscopy

Xiao-Miao Zhao,<sup>1,2</sup> Qiao-Wei Huang,<sup>1,2</sup> Jiang Zhang,<sup>1</sup> Guo-Hua Zhong,<sup>3</sup> Hai-Qing Lin,<sup>4</sup> and Xiao-Jia Chen<sup>2,5,a)</sup>

<sup>1</sup>Department of Physics, South China University of Technology, Guangzhou 510640, China

<sup>2</sup>Center for High Pressure Science and Technology Advanced Research, Shanghai 201203, China

<sup>3</sup>Center for Photovoltaics and Solar Energy, Shenzhen Institutes of Advanced Technology, Chinese Academy of Sciences, Shenzhen 518055, China

<sup>4</sup>Beijing Computational Science Research Center, Beijing 100084, China

<sup>5</sup>Geophysical Laboratory, Carnegie Institution of Washington, Washington, DC 20015, USA

(Received 29 January 2014; accepted 13 June 2014; published online 30 June 2014)

Vibrational properties of isoviolanthrone are investigated by Raman scattering at pressures up to 30.5 GPa and room temperature. A complete characterization of phonon spectra under pressure is given for this material. The onset of a phase transition at 11.0 GPa and the formation of a new phase above 13.8 GPa are identified from both the frequency shifts and the changes in the full width half maxima of the intra- and internal modes. The transition is proposed to result from the changes of intra- and intermolecular bonding. The tendencies of the intensity ratios with pressure are in good agreement with the pressure dependence of the resistance at room temperature, indicating that the phase transition may be an electronic origin. The absence of the changes in the lattice modes indicates that the observed phase transition is probably a result of the structural distortions or reorganizations. The reversible character of the transition upon compression and decompression is determined in the entire pressure region studied. © 2014 AIP Publishing LLC. [<http://dx.doi.org/10.1063/1.4885142>]

### I. INTRODUCTION

Isoviolanthrone with “armchair” molecular structure has similar optical and electronic properties to polycyclic aromatic hydrocarbons (PAHs).<sup>1,2</sup> The PAHs’ electronic structure with  $\pi$  electron networks can be modified by metal doping, which can bring out novel physical properties, such as superconductivity.<sup>3–7</sup> With increasing the length of the PAHs chain, the superconductor transition temperature ( $T_c$ ) increases dramatically from 5 K for K<sub>3</sub>phenanthrene with three benzene rings to 33 K for K<sub>3,45</sub>dibenzopentacene with seven benzene rings. Kato *et al.*<sup>8</sup> reported that molecular edge structures as well as molecular sizes have relevance to the strength of electron-phonon coupling and  $T_c$ s. Furthermore, pressure-induced semi-conductivity in isoviolanthrone with nine benzene rings is found in high pressure phase from electrical resistance measurements and the resistance is on the order of 50.<sup>1</sup> The pressure effect of such PAHs superconductors is remarkable where the  $T_c$  of K<sub>3</sub>picene (18 K phase) increases linearly with pressure up to 1.2 GPa with  $dT_c/dP = 12.5$  K GPa<sup>-1</sup>,<sup>9</sup> additionally, within the phenanthrene based superconductors, Wang *et al.*<sup>4</sup> showed that  $T_c$  was enhanced by the application of pressure. In some cases, pressure may even be the decisive parameter in achieving superconductivity such as the highest  $T_c$  of 38 K observed in Cs<sub>3</sub>C<sub>60</sub>.<sup>10</sup> Thus, the application of pressure is of paramount importance to explore superconductivity within organic systems. Because both the increase of the length of the PAHs chain and the application of pressure are two favorable factors for enhancing superconductivity in such systems, isoviolanthrone is considered as an

ideal system for achieving higher  $T_c$  if it eventually becomes superconductive upon chemical doping or pressure. The high-pressure behavior of this material with long benzene chain is becoming attractive from the viewpoint of exploring high-temperature superconductivity.

Understanding pressure effect on organic compounds is important for synthesizing, designing, and discovering materials with higher  $T_c$ 's at ambient pressure. Isoviolanthrone, the molecules of which consist of condensations of benzene rings resembling that in the graphite layers and two C=O bonds (Fig. 1), which has been described previously.<sup>11</sup> Natural isoviolanthrone possesses monoclinic symmetry with four molecules per unit cell, the space group  $P2_1/c$  and lattice parameters:  $a = 15.210$  Å,  $b = 3.825$  Å,  $c = 33.120$  Å,  $\beta = 90.8^\circ$  and  $V = 1926.68$  Å<sup>3</sup>. The molecular packing is of the stacked ploughshare type. In an early study where the effect of pressure to several hundred kilobars has been measured on the resistance of seven-fused ring aromatic compound, including two polyacenes and five quinones, indicating that the conductivity increase with molecular size and the resistance of isoviolanthrone is lower than polyacenes at high pressures.<sup>1</sup> Extensive investigations on other polyacenes have showed that pentacene, a straight-chain aromatic hydrocarbon, exhibited metallic character with a positive temperature coefficient of resistance at 27 GPa.<sup>12</sup> Therefore, the investigation of isoviolanthrone under pressure is of great importance to discovering new materials with higher  $T_c$ 's at ambient pressure. Furthermore, theoretical studies have attempted to investigate the electron-phonon interactions as a possible nature of superconductivity in PAHs.<sup>13–15</sup> Knowledge of the physics and vibrational properties of isoviolanthrone at high pressures is helpful to understand the electron-phonon

<sup>a)</sup>Electronic mail: xjchen@hpstar.ac.cn

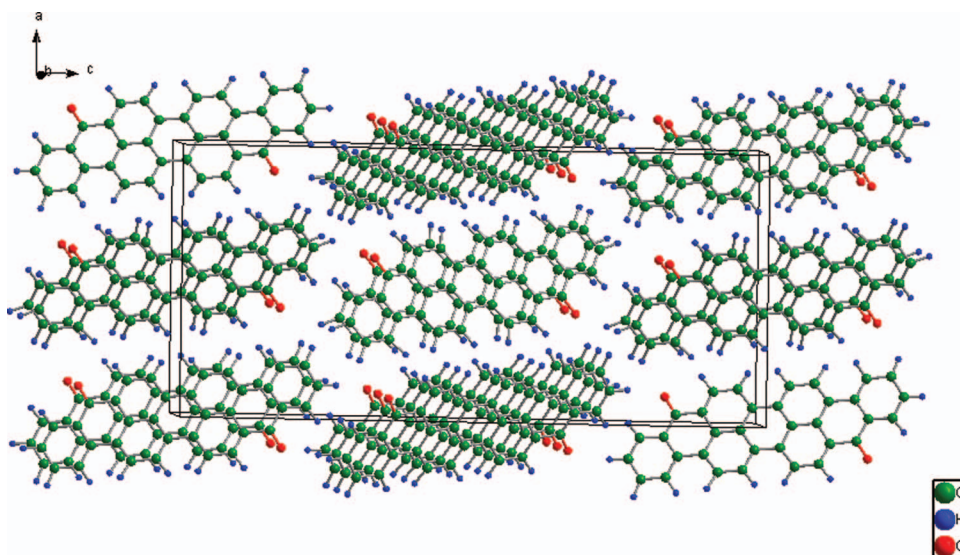


FIG. 1. Crystal structure of pristine solid isoviolanthrone, solid lines delineate unit cells.

coupling. In order to understand the intermolecular interaction and electron-phonon interaction of isoviolanthrone, a thorough study focused on the molecular vibrational properties of isoviolanthrone under pressure is highly desirable.

In this paper, we perform high-pressure Raman scattering measurements on isoviolanthrone up to 30.5 GPa at room temperature. The results reveal the onset of a phase transition at 11.0 GPa and the formation of the new phase above 13.8 GPa. On the basis of the change in the Raman spectra obtained in both compression and decompression runs, we analyze the tendencies of the intensity ratio, which are in good agreement with the results of the resistance at high pressures and room temperature, indicating that the phase transition is probably an electronic origin. The transition of isoviolanthrone upon compression and decompression is found to be entirely reversible in the pressure region studied.

## II. EXPERIMENTAL DETAILS

Isoviolanthrone (99.9% purity) was purchased from TCI Co. and used without further purification. High-pressure Raman experiments were carried out by using a diamond anvil cell with beveled anvils with a 400  $\mu\text{m}$  culet. The hole of the gasket serving as the sample chamber was set to about 130  $\mu\text{m}$  in diameter and 50  $\mu\text{m}$  in thickness. To avoid chemical reaction, no pressure medium was used for isoviolanthrone. The pressure was determined from the shift of the luminescence spectrum of a ruby chip enclosed in the sample.<sup>16</sup> The ruby  $R_1$  and  $R_2$  line splitting was used found to remain almost constant up to 16 GPa, showing that the compression in our experiment is hydrostaticity below 16 GPa. Renishaw Invia Raman system with a spectrometer (with 1800 lines/mm grating) was used for the measurement, giving a resolution of 1  $\text{cm}^{-1}$ . The Raman spectra were measured in backscattering geometry with visible laser excitation (532 nm) with power less than 50 mW. The illuminated spot for the Raman measurements was less than 5  $\mu\text{m}$  in size. All the spectra were

measured at room temperature. The spectra were collected from 100 to 3500  $\text{cm}^{-1}$ .

## III. RESULTS AND DISCUSSION

Raman scattering, which measures phonons (lattice and molecular vibrations) in Brillouin zone center, possesses a very high selectivity and is known to be a powerful technique for the investigation of both chemical reactivity and even subtle structural distortion both within a space group (via band shifts) and due to phase transitions (via band splitting and/or soft modes). The crystal structure and molecular structure of isoviolanthrone are shown in Fig. 1. Based on the analysis of molecular structure, it is clear that the Raman spectra of isoviolanthrone consist of both the vibrations of polycyclic aromatic hydrocarbon and the C=O vibration. In the present study, we have measured the Raman spectrum within the region from 100 to 3500  $\text{cm}^{-1}$  as a function of pressure up to 30.5 GPa. No theoretical calculations and experimental data about Raman spectra at ambient pressure have ever been reported in the literature, so the symmetries of the Raman modes are indefinite. On the basis of the Raman spectra obtained for both compression and decompression processes, we found that the vibrational properties of the studied material are similar to those of the parent PAHs based superconductors.<sup>17–20</sup> Table I summarizes the measured modes at ambient conditions and assignment.<sup>21,22</sup>

Figure 2 shows the Raman spectra obtained for isoviolanthrone at various pressures up to 30.5 GPa in the region from 120 to 1230  $\text{cm}^{-1}$  at room temperature. It should be noted that the intensities of the vibrational modes drastically decrease when pressure is increased up to 13.2 GPa, accompanied with the increasing fluorescence background. One can clearly see that the lattice modes  $L_1$  and  $L_2$  are separated from each other at ambient pressure, when the pressure is increased to 11.0 GPa, their Raman frequencies are close to each other and then combine into a broad peak above 13.2 GPa where the new peak may be a superposition of the two mode excitations. It

TABLE I. Raman modes and their assignments from Refs. 21 and 22 for isoviolanthrone.

| Raman modes    | Assignment                 | Observed (cm <sup>-1</sup> ) | Raman modes | Assignment               | Observed (cm <sup>-1</sup> ) |
|----------------|----------------------------|------------------------------|-------------|--------------------------|------------------------------|
| L <sub>1</sub> | Lattice mode               | 193                          | $\nu_{29}$  | Aromatic C–C stretching  | 1467                         |
| L <sub>2</sub> | Lattice mode               | 218                          | $\nu_{30}$  | Aromatic C–C stretching  | 1486                         |
| $\nu_1$        | C–C–C out-of-plane Bending | 333                          | $\nu_{31}$  | Aromatic C–C stretching  | 1509                         |
| $\nu_2$        | C–C–C out-of-plane Bending | 378                          | $\nu_{32}$  | Aromatic C–C stretching  | 1522                         |
| $\nu_3$        | C–C–C out-of-plane Bending | 389                          | $\nu_{33}$  | Aromatic C–C stretching  | 1564                         |
| $\nu_4$        | C–C–C out-of-plane Bending | 418                          | $\nu_{34}$  | Aromatic C–C stretching  | 1577                         |
| $\nu_5$        | C–C–C out-of-plane Bending | 434                          | $\nu_{35}$  | Aromatic C–C stretching  | 1594                         |
| $\nu_6$        | C–C–C out-of-plane Bending | 465                          | $\nu_{36}$  | Aromatic C–C stretching  | 1603                         |
| $\nu_7$        | C–C–C out-of-plane Bending | 487                          | $\nu_{37}$  | Aromatic C–C stretching  | 1613                         |
| $\nu_8$        | C–C–C out-of-plane Bending | 516                          | $\nu_{38}$  | –C=O stretching          | 1648                         |
| $\nu_9$        | C–C–C out-of-plane Bending | 532                          | $\nu_{39}$  | Overtone or combinations | 1760                         |
| $\nu_{10}$     | C–C–C out-of-plane Bending | 558                          | $\nu_{40}$  | Overtone or combinations | 1794                         |
| $\nu_{11}$     | C–H out-of-plane Bending   | 638                          | $\nu_{41}$  | Overtone or combinations | 1814                         |
| $\nu_{12}$     | C–H out-of-plane Bending   | 658                          | $\nu_{50}$  | Aromatic C–H stretching  | 2558                         |
| $\nu_{13}$     | C–H out-of-plane Bending   | 789                          | $\nu_{51}$  | Aromatic C–H stretching  | 2579                         |
| $\nu_{14}$     | C–H out-of-plane Bending   | 814                          | $\nu_{52}$  | Aromatic C–H stretching  | 2614                         |
| $\nu_{15}$     | C–H out-of-plane Bending   | 933                          | $\nu_{53}$  | Aromatic C–H stretching  | 2653                         |
| $\nu_{16}$     | C–H out-of-plane Bending   | 992                          | $\nu_{54}$  | Aromatic C–H stretching  | 2575                         |
| $\nu_{17}$     | C–H in plane Bending       | 1039                         | $\nu_{55}$  | Aromatic C–H stretching  | 2714                         |
| $\nu_{18}$     | C–H in plane Bending       | 1046                         | $\nu_{56}$  | Aromatic C–H stretching  | 2748                         |
| $\nu_{19}$     | C–H in plane Bending       | 1060                         | $\nu_{57}$  | Aromatic C–H stretching  | 2765                         |
| $\nu_{20}$     | C–H in plane Bending       | 1127                         | $\nu_{58}$  | Aromatic C–H stretching  | 2844                         |
| $\nu_{21}$     | C–H in plane Bending       | 1176                         | $\nu_{59}$  | Aromatic C–H stretching  | 2865                         |
| $\nu_{22}$     | C–H in plane Bending       | 1200                         | $\nu_{60}$  | Aromatic C–H stretching  | 2902                         |
| $\nu_{23}$     | C–H in plane Bending       | 1249                         | $\nu_{61}$  | Aromatic C–H stretching  | 2937                         |
| $\nu_{24}$     | Aromatic C–C stretching    | 1279                         | $\nu_{62}$  | Aromatic C–H stretching  | 3028                         |
| $\nu_{25}$     | Aromatic C–C stretching    | 1301                         | $\nu_{63}$  | Aromatic C–H stretching  | 3089                         |
| $\nu_{26}$     | Aromatic C–C stretching    | 1375                         | $\nu_{64}$  | Aromatic C–H stretching  | 3130                         |
| $\nu_{27}$     | Aromatic C–C stretching    | 1422                         | $\nu_{65}$  | Aromatic C–H stretching  | 3154                         |
| $\nu_{28}$     | Aromatic C–C stretching    | 1457                         |             |                          |                              |

is worth noting that two weak peaks of  $\nu_2$  and  $\nu_3$  corresponding to C–C–C out of plane bending show increase in intensity with the increasing pressure and merge into a single peak at 13.2 GPa. Furthermore, it is noteworthy to mention that the  $\nu_2$  and  $\nu_3$  Raman bands are very strong and very sharp at ambient pressure and then combine into a single peak at pressures above 12.0 GPa which is coupled with the internal mode of  $\nu_{11}$ . More interestingly, the intensity of the  $\nu_{14}$  increases with increasing pressure. However, the intensity of the strong peak  $\nu_{20}$  (with  $E_{1g}$  symmetry) decreases and is lower than  $\nu_{14}$  (with  $E_{2g}$  symmetry) at 12.0 GPa. This behavior indicates the exchange of the symmetry of the modes and may result from Fermi resonance.<sup>23</sup> The disappearance of bands, overlapping peaks, and the change of the intensities of peaks together contribute to the formation of a new phase above 13.2 GPa.

Figure 3 shows the Raman spectra of isoviolanthrone at various pressures up to 30.5 GPa in the range between 1230 and 1800 cm<sup>-1</sup>. When the pressure is increased to 13.8 GPa, the Raman vibrational pattern behaves differently from the spectra at ambient pressure. The intensity of the mode  $\nu_{33}$  is much stronger than the mode  $\nu_{36}$  at ambient pressure, however, the mode  $\nu_{36}$ , associated with aromatic C–C stretching, gains intensity rapidly as pressure is increased and is as strong as the intensity of the mode  $\nu_{33}$  above 13.8 GPa. In addition, the modes of  $\nu_{23}$  and  $\nu_{28}$  disappear and the intramolecular mode (originally at 1375 cm<sup>-1</sup>) shows a

substantial broadening at this pressure. The dramatic change in intensity and the disappearance of the internal modes provide further evidence of phase transformation at this pressure range. As can be seen in Fig. 4, all the Raman peaks become broaden, accompanied with the significantly increasing fluorescence background. The Raman bands are generally broadened. This is probably a result of the rotations and molecular interactions (vibrational relaxation). Additionally, the modes of  $\nu_{43}$  and  $\nu_{44}$  vanish at 11.0 GPa, indicating the onset of a phase transition. The occurrence of fluorescence may also result from the shortened distance between molecules at high pressures where one may observe orbital overlap between two adjacent  $\pi$ -conjugated molecules (creating a new molecular orbital across two molecules),<sup>24</sup> or from excited structural defects similar to coronene.<sup>17</sup>

In order to precisely determine the pressure at which phase transitions take place, we plotted the pressure dependencies of Raman modes in detail. As seen in Fig. 5, the internal modes of  $\nu_6$ ,  $\nu_7$ , and  $\nu_{11}$  disappear as pressure is increased up to 13.2 GPa and a shoulder appears on the high-frequency side of  $\nu_{13}$  at 11.0 GPa. In addition, the shoulder band exhibits a negative frequency shift, indicating weakened intramolecular bonding and enhanced intermolecular interaction. This slight softening against pressure may arise from the rotation of molecular. It is noteworthy to mention that the lattice modes of L<sub>1</sub> and L<sub>2</sub> begin to close to each other from

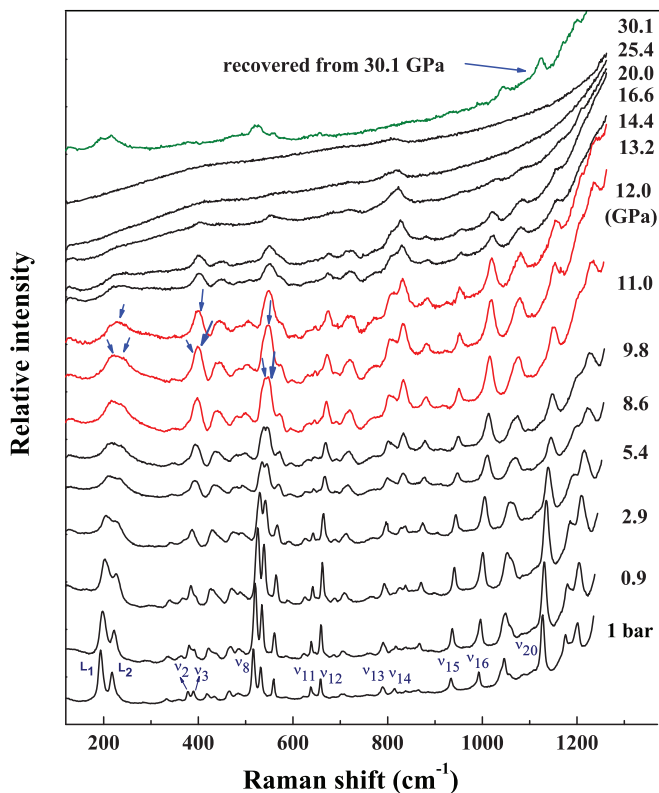


FIG. 2. Representative Raman spectra of isoviolanthrone in the low frequency range of 100–1250  $\text{cm}^{-1}$  at various pressures up to 30.1 GPa and decompressed from 30.5 GPa. The arrows indicate the changes of Raman modes.

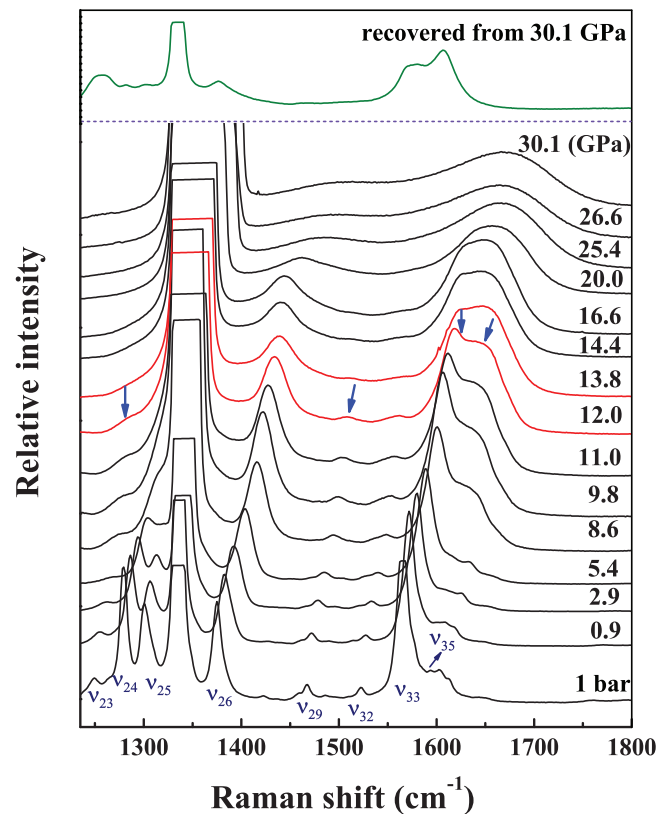


FIG. 3. Selected Raman spectra of isoviolanthrone in the frequency range of 1200–1800  $\text{cm}^{-1}$  at various pressures up to 30.1 GPa and decompressed from 30.5 GPa. The arrows indicate the changes of Raman modes.

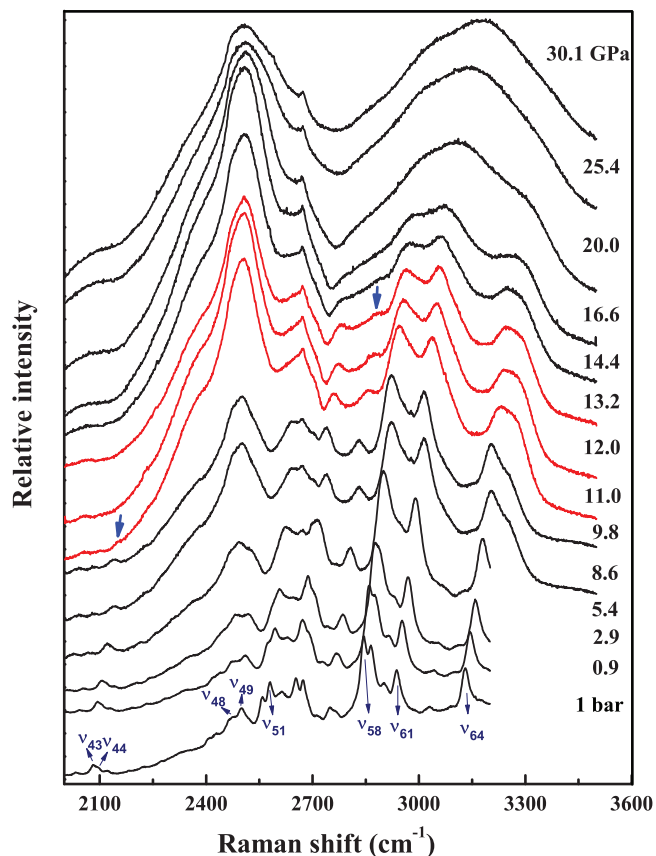


FIG. 4. Raman spectra obtained for solid isoviolanthrone up to 30.1 GPa in the high frequency range of 2000–3500  $\text{cm}^{-1}$ . The arrows indicate the changes of Raman modes.

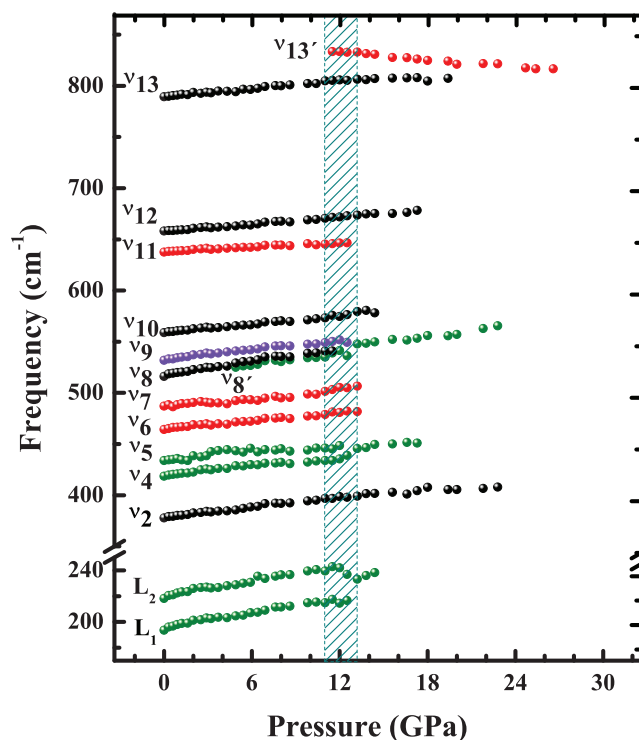


FIG. 5. Pressure dependence of vibrational frequencies observed of isoviolanthrone in the low frequency range of 100–900  $\text{cm}^{-1}$  at room temperature. The pressure range for the sudden changes in the Raman spectra is indicated by shading

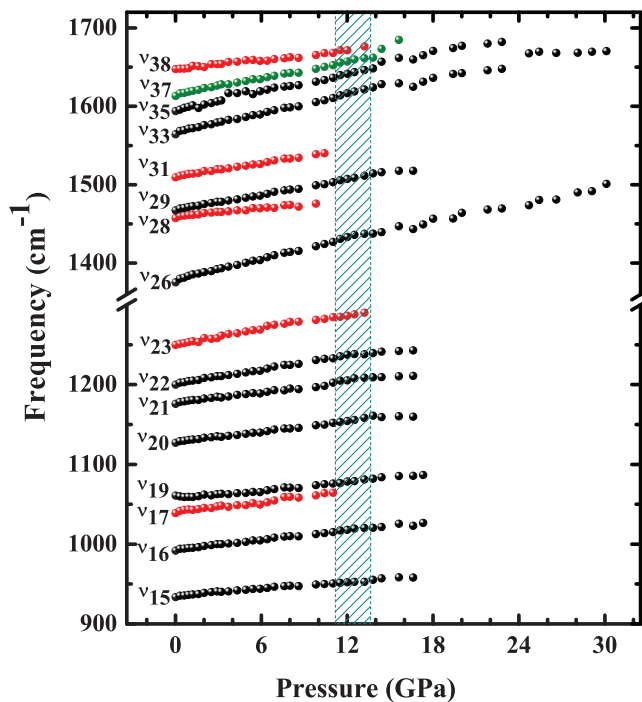


FIG. 6. Pressure-induced Raman frequency shift of several vibrons of crystalline isoviolanthrone at room temperature. The marked area and vertical dashed lines indicate the phase boundaries.

11.0 GPa and overlap above 13.2 GPa, meanwhile, the internal modes of  $\nu_4$  and  $\nu_5$  exhibit the similar behavior, indicating the onset of a phase transition at 11.0 GPa and the formation of another phase above 13.2 GPa. We now focus our attention on higher frequencies region (see Fig. 6). The significant changes of higher frequencies can also be observed as pressure is increased. Several vibrational modes of  $\nu_{17}$ ,  $\nu_{28}$ , and  $\nu_{31}$  disappear at approximately 11.0 GPa and then the  $\nu_{23}$  and  $\nu_{38}$  bands vanish at 13.2 GPa. The peak of  $\nu_{37}$  exhibits sudden change of slope at 13.8 GPa, implying that a phase transition may take place at this point. Figure 7 shows the pressure dependence of the peak position of isoviolanthrone in the range between 2000 and 3500  $\text{cm}^{-1}$ . In this region, obvious discontinuities in the pressure shift and changes in the rate of shift versus pressure were exhibited at 11.0 GPa. Furthermore, the internal modes of  $\nu_{43}$ ,  $\nu_{44}$ , and  $\nu_{51}$  vanish at this point. It is worth noting that a shoulder appears on the high-frequency side of  $\nu_{56}$  at 11.0 GPa and then the peak  $\nu_{56}$  disappears at 13.2 GPa, providing further evidence of a narrow transition phase range of only 2.2 GPa from 11.0 GPa to 13.2 GPa.

Figure 8 shows the pressure dependence of full width half maximum (FWHM) of selected vibrational modes. The FWHM of vibrational modes  $\nu_{20}$  and  $\nu_{26}$  has a relative small value in the low-pressure region, however, broaden abruptly with increasing pressure at pressure near the phase transition of 11.0 GPa. Upon further compression to 13.2 GPa, the FWHM of vibrational modes  $\nu_{12}$  and  $\nu_{16}$  shows a sudden increase with increasing pressure. The pressure-induced FWHM narrowing of the lattice mode  $L_1$  is similar to the behavior of anthracene under pressure.<sup>25</sup> It can be interpreted that the pressure-induced FWHM narrowing may reflect decreased homogeneous dephasing due to decrease in phonon

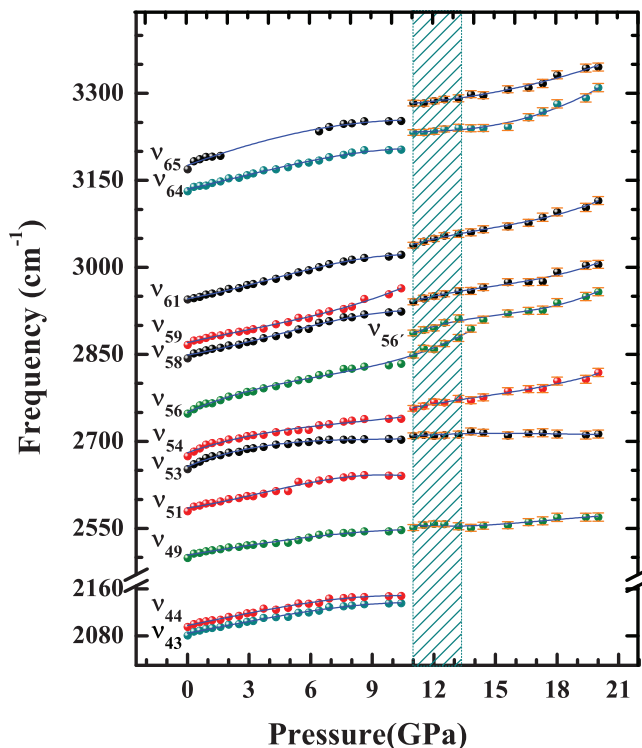


FIG. 7. Vibrational frequency plotted as a function of pressure in the high frequency range of 2000–3500  $\text{cm}^{-1}$ . The solid lines are drawn to guide the eye, error bars indicated for all pressure where the least squares fitting of the band profile carries smaller uncertainties than average. The shadow area and vertical dashed lines indicate the phase boundaries.

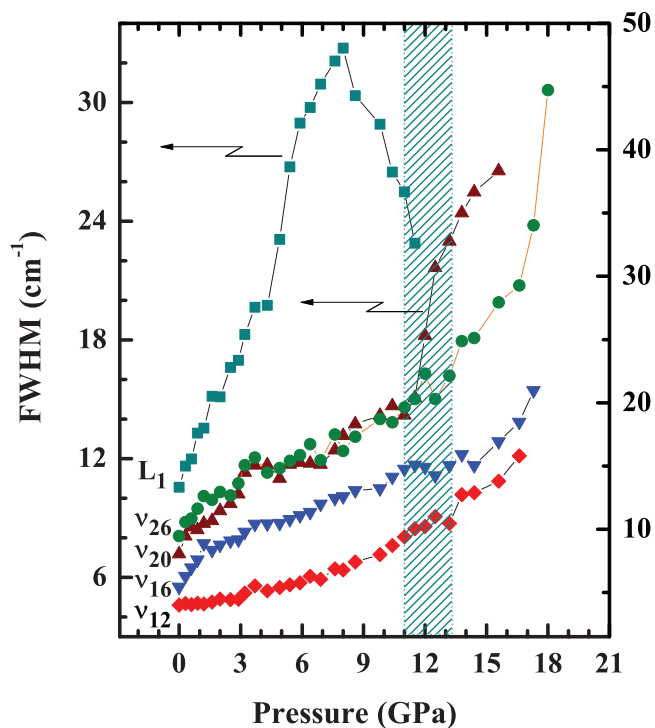


FIG. 8. Full width maximum (FWHM) of selected vibrational modes of isoviolanthrone as a function of pressure from ambient pressure to 30.5 GPa. The shadow area and vertical dashed lines indicate the phase boundaries.

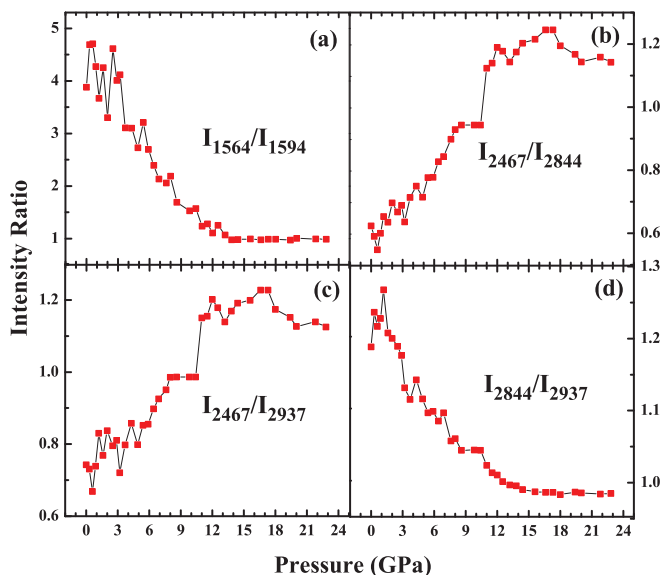


FIG. 9. Pressure dependence of Raman intensity ratio between the Raman bands: (a) 1564–1594  $\text{cm}^{-1}$ , (b) 2467–2844  $\text{cm}^{-1}$ , (c) 2467–2937  $\text{cm}^{-1}$ , and (d) 2844–2937  $\text{cm}^{-1}$ .

occupation numbers caused by the pressure-induced increase in phonon energies. As is well-known, electron-phonon coupling constant ( $\lambda$ ) is closely connected with the vibrational properties. According to previous report about  $\text{Cs}_3\text{C}_{60}$ ,<sup>26</sup> the relationship between the electron-phonon coupling  $\lambda_i$  and the line width  $\tau_i$  is roughly linear, where  $\lambda_i$  is the contribution to  $\lambda$  from the  $i$ th mode. Thus, the molecule isoviolanthrone may possess an enhanced electron-phonon coupling constant above 13.2 GPa since almost all the vibrational modes become broader with increasing pressure.

Figure 9 shows the Raman intensity ratios for some selected internal bands as a function of pressure. One can clearly see that the inflexions of the tendencies are found around 13.8 GPa. This behavior is quite suggestive to imply that the change of the signal intensity ratio should be simply associated to a few modifications of molecular configuration, which is consistent with the phase transition at around 13.8 GPa. The similar behavior of Raman band intensities was also observed for the pressure-induced phase transition.<sup>24,27</sup> The intensity ratios of  $I_{2467/2844}$  and  $I_{2497/2937}$  are greater than 1 above 12.0 GPa, which is possibly due to the exchange of the symmetry of the modes and may also be due to the unsaturated carbon converting into saturated carbon under applied pressure. More interestingly, the tendencies of the intensity ratios of  $I_{1564/1594}$  and  $I_{2844/2937}$  are in good agreement with the results of the resistance at ambient temperature. There is a sharp drop in resistance in the low-pressure region, and then the drop is slowed down only by a factor of 3.5 between 200 and 300 kilobars and by 1.5 over the range 300–500 kilobars.<sup>1</sup> On the basis of above analysis, we can reasonably speculate that the phase transition is probably an electron phase transition. The different critical pressure between the Raman and resistance measurements may be a result of the longer transient phase during the resistance measurement.

According to the Raman spectroscopy results, both the disappearance of internal modes and the overlapping of sev-

eral peaks provide evidence for higher symmetry above 13.8 GPa. However, because of the absence of the changes of both the lattice modes and additional XRD diffraction patterns, the observed changes may originate from the possible structural distortion or reorganizations. As can be seen in Figs. 2 and 3, most Raman modes are reversible when decompressed from 30.5 GPa except for the exchange of the intensity of some peaks. It can be inferred that the bands of big molecular size have a relatively high stability with respect to other organic compound such as coronene, phenanthrene, or picene. It is expected from the previous reports that within a given family of compounds, the conductivity should increase with molecular size, the molecule of isoviolanthrone may be a potential metal or even superconductor at high pressure and low temperature, accompanied with an enhanced electron-phonon coupling constant at high pressures.

#### IV. CONCLUSIONS

In summary, we have investigated the vibrational properties of isoviolanthrone at high pressures up to 30.5 GPa by Raman scattering measurements at room temperature. Our study provides a complete characterization of phonon spectra of this material. The experimental results revealed the onset of a phase transition at 11.0 GPa and the formation of the new phase above 13.8 GPa from both the disappearance of intra- and internal modes and the change in the full width half maxima of internal modes. The transition was suggested to result from the changes of intra- and intermolecular bonding of this material. The tendencies of the intensity ratio are in good agreement with the results of the resistance at room temperature, indicating that the phase transition may be an electronic origin. The molecule isoviolanthrone possibly possesses an enhanced electron-phonon coupling constant above 13.2 GPa. The transition of isoviolanthrone upon compression and decompression was entirely reversible in the pressure region studied. There are no changes in the lattice modes, the phase transition observed from Raman changes was proposed to originate from the structural distortions or reorganizations. It is desirable that the present observation about vibrational properties will motivate further theoretical and experimental investigations for a better understanding of the family of organic compounds and offer ideas of synthesizing and discovering materials with higher  $T_c$ .

#### ACKNOWLEDGMENTS

This work was supported by the Cultivation Fund of the Key Scientific and Technical Innovation Project Ministry of Education of China (No. 708070), the Shenzhen Basic Research Grant (No. JC201105190880A), the National Natural Science Foundation of China (No. 11274335), and the Fundamental Research Funds for the Central Universities SCUT (No. 2014ZZ0069).

<sup>1</sup>G. A. Samara and H. G. Drickamer, *J. Chem. Phys.* **37**, 474 (1962).

<sup>2</sup>H. Inokuchi, *Bull. Chem. Soc. Jpn.* **28**, 8 (1955).

<sup>3</sup>R. Mitsuhashi, Y. Suzuki, Y. Yamanari, H. Mitamura, T. Kambe, N. Ikeda, H. Okamoto, A. Fujiwara, M. Yamaji, N. Kawasaki, Y. Maniwa, and Y. Kubozono, *Nature* **464**, 76 (2010).

- <sup>4</sup>X. F. Wang, R. H. Liu, Z. Gui, Y. L. Xie, Y. J. Yan, J. J. Ying, X. G. Luo, and X. H. Chen, *Nat. Commun.* **2**, 507 (2011).
- <sup>5</sup>Y. Kubozono, H. Mitamura, X. Lee, X. He, Y. Yamanari, Y. Takahashi, Y. Suzuki, Y. Kaji, R. Eguchi, K. Akaike, T. Kambe, H. Okamoto, A. Fujiwara, T. Kato, T. Kosugi, and H. Aoki, *Phys. Chem. Chem. Phys.* **13**, 16476 (2011).
- <sup>6</sup>M. Q. Xue, T. B. Cao, D. M. Wang, Y. Wu, H. X. Yang, X. L. Dong, J. B. He, F. W. Li, and G. F. Chen, *Sci. Rep.* **2**, 389 (2012).
- <sup>7</sup>Q. W. Huang, G. H. Zhong, J. Zhang, X. M. Zhao, C. Zhang, H. Q. Lin, and X. J. Chen, *J. Chem. Phys.* **140**, 114301 (2014).
- <sup>8</sup>T. Kato, K. Yoshizawa, and K. Hirao, *J. Chem. Phys.* **116**, 3420 (2002).
- <sup>9</sup>T. Kambe, X. He, Y. Takahashi, Y. Yamanari, K. Teranishi, H. Mitamura, S. Shibasaki, K. Tomita, R. Eguchi, H. Goto, Y. Takabayashi, T. Kato, A. Fujiwara, T. Kariyado, H. Aoki, and Y. Kubozono, *Phys. Rev. B* **86**, 214507 (2012).
- <sup>10</sup>A. Y. Ganin, Y. Takabayashi, Y. Z. Khimyak, S. Margadonna, A. Tamal, M. J. Rosseinsky, and K. Prassides, *Nat. Mater.* **7**, 367 (2008).
- <sup>11</sup>W. Bolton, *Acta Cryst.* **17**, 1020 (1964).
- <sup>12</sup>R. B. Aust, W. H. Bentley, and H. G. Drickamer, *J. Chem. Phys.* **41**, 1856 (1964).
- <sup>13</sup>M. Casula, M. Calandra, G. Profeta, and F. Mauri, *Phys. Rev. Lett.* **107**, 137006 (2011).
- <sup>14</sup>A. Subedi and L. Boeri, *Phys. Rev. B* **84**, 020508(R) (2011).
- <sup>15</sup>T. Kato, T. Kambe, and Y. Kubozono, *Phys. Rev. Lett.* **107**, 077001 (2011).
- <sup>16</sup>H. K. Mao, P. M. Bell, J. W. Shaner, and D. J. Stembey, *J. Appl. Phys.* **49**, 3276 (1978).
- <sup>17</sup>X. M. Zhao, J. Zhang, A. Berlie, Z. X. Qin, Q. W. Huang, J. Shan, J. B. Zhang, L. Y. Tang, J. Liu, C. Zhang, G. H. Zhong, H. Q. Lin, and X. J. Chen, *J. Chem. Phys.* **139**, 144308 (2013).
- <sup>18</sup>Q. W. Huang, J. Zhang, A. Berlie, Z. X. Qin, X. M. Zhao, J. B. Zhang, L. Y. Tang, J. Liu, C. Zhang, G. H. Zhong, H. Q. Lin, and X. J. Chen, *J. Chem. Phys.* **139**, 104302 (2013).
- <sup>19</sup>S. Fanetti, M. Citroni, L. Malavasi, G. A. Artioli, P. Postorino, and R. Bini, *J. Phys. Chem. C* **117**, 5343 (2013).
- <sup>20</sup>F. Capitani, M. Höppner, B. Joseph, L. Malavasi, G. A. Artioli, L. Baldassarre, A. Perucchi, M. Piccinini, S. Lupi, P. Boeri, and P. Postorino, *Phys. Rev. B* **88**, 144303 (2013).
- <sup>21</sup>L. Colangeli, V. Mennella, G. A. Baratta, E. Bussoletti, and G. Strazzulla, *Astrophys. J.* **396**, 369 (1992).
- <sup>22</sup>E. Smith and G. Dent, *Modern Raman Spectroscopy: A Practical Approach* (John Wiley and Sons Ltd, England, 2005).
- <sup>23</sup>Y. Lin, W. L. Mao, V. Drozd, J. H. Chen, and L. L. Daemen, *J. Chem. Phys.* **129**, 234509 (2008).
- <sup>24</sup>X. D. Tang, Z. J. Ding, and Z. M. Zhang, *Solid State Commun.* **149**, 301 (2009).
- <sup>25</sup>L. Zhao, B. J. Baer, and E. L. Chronister, *J. Phys. Chem.* **103**, 1728 (1999).
- <sup>26</sup>S. Fujiki, Y. Kubozono, S. Emura, Y. Takabayashi, S. Kashino, A. Fujiwara, K. Ishii, H. Suematsu, Y. Murakami, Y. Iwasa, T. Mitani, and H. Ogata, *Phys. Rev. B* **62**, 5366 (2000).
- <sup>27</sup>A. Teixeira, P. Freire, A. Moreno, J. Sasaki, A. Ayala, J. M. Fijo, and F. Melo, *Solid State Commun.* **116**, 405 (2000).